Journal of Organometallic Chemistry, 437 (1992) 347–361
Elsevier Sequoia S.A., Lausanne
JOM 22764

Triosmium carbonyl cluster complexes of bridging phosphonate, arsonate, and phosphinate ligands

Greg R. Frauenhoff, Jia-Chu Liu, Scott R. Wilson and John R. Shapley
School of Chemical Sciences and Materials Research Laboratory, University of Illinois, Urbana, Illinois 61801 (USA)

(Received December 13, 1991)

Abstract

Treatment of $(\mu\text{-H})_3Os_3(CO)_9(\mu_3\text{-CH})$ sequentially with trifluoromethanesulfonic acid followed by a phosphonic or arsonic acid provides compounds of the formula $(\mu\text{-H})_2Os_3(CO)_9(\mu_3,\eta^3\text{-}O_3ER)$ [E = P, R = Ph(**3**), Me(**4**); E = As, R = Ph(**5**)]. Assignments of important infrared bands for the coordinated oxyanions have been made. The complex $(\mu\text{-H})_2Os_3(CO)_9(\mu_3,\eta^3\text{-}O_3PPh)$ (**3**) has been studied by variable temperature ^{13}C NMR spectroscopy. The reaction of $Os_3(CO)_{10}(S)_2$ (S = C_8H_{14},CH_3CN) with Ph_2PO_2H in THF at 55–60°C produces $(\mu\text{-H})Os_3(CO)_{10}(\mu,\eta^2\text{-}O_2PPh_2)$ (*ca.* 60%), the structure of which has been determined by X-ray crystallography.

Introduction

The synthesis and characterization of the oxyanion cluster complexes $(\mu\text{-H})_2Os_3(CO)_9(\mu_3,\eta^3\text{-}O_3SO)$ (**1**) and $(\mu\text{-H})_2Os_3(CO)_9(\mu_3,\eta^3\text{-}O_3POH)$ (**2**) have been described previously [1]. We have extended the methodology used in preparing the purely inorganic derivatives **1** and **2** to the synthesis of tridentate phosphonate ($(\mu\text{-H})_2Os_3(CO)_9(\mu_3,\eta^3\text{-}O_3PR)$, R = Ph (**3**), Me (**4**)) and arsonate ($(\mu\text{-H})_2Os_3(CO)_9(\mu_3,\eta^3\text{-}O_3AsPh)$ (**5**)) derivatives, which are described in this paper. Although there are several structurally characterized molecular examples of triply bridging tridentate coordination for both sulfate [1,2] and phosphate [3], tridentate coordination of phosphonate (and arsonate) groups in molecular polyoxoanions frequently shows bridging interactions to more than three metal atoms [4]; however, triply bridging coordination is thought to occur in layered zirconium phosphonates [5].

Compounds **1–5** may be appropriate models for oxyanion adsorption on surfaces [6]. A tridentate methylphosphonate species has been discussed in studies of the chemisorption of dimethyl(methylphosphonate) on both γ-alumina [7] and

---

Correspondence to: Dr. J.R. Shapley.

platinum [8] and similar species may be involved in oxyanion adsorption on metal electrode surfaces [9].

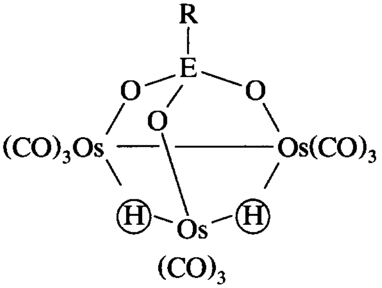

1: $O_3ER = O_3SO$
2: $O_3ER = O_3POH$
3: $O_3ER = O_3PPh$
4: $O_3ER = O_3PMe$
5: $O_3ER = O_3AsPh$

Here we also report the synthesis and structure of the bidentate, bridging phosphinate ligand complex $(\mu\text{-H})Os_3(CO)_{10}(\mu,\eta^2\text{-}O_2PPh_2)$.

Results and discussion

Synthesis and characterization of compounds 3–5

We have reported previously that $(\mu\text{-H})_3Os_3(CO)_9(\mu_3\text{-CH})$ [10] "dissolves" in H_2SO_4 with the evolution of gas (predominantly methane) and the formation of $(\mu\text{-H})_2Os_3(CO)_9(\mu_3,\eta^3\text{-}O_3SO)$ (**1**) [1]. No corresponding reaction with H_3PO_4 was observed. However, $(\mu\text{-H})_2Os_3(CO)_9(\mu_3,\eta^3\text{-}O_3POH)$ (**2**) can be prepared by first dissolving $(\mu\text{-H})_3Os_3(CO)_9(\mu_3\text{-CH})$ in neat F_3CSO_3H, with concomitant gas evolution, followed by addition of H_3PO_4 [1]. In work reported elsewhere, we have isolated a neutral species of formula $H_2Os_3(CO)_9(O_3SCF_3)_2$ from such solutions in high yield [11]. We have extended this methodology to the synthesis of phosphonate and arsonate derivatives. In each case, addition of excess free acid to the F_3CSO_3H solution gave mixtures from which **3**–**5** could be isolated in low to poor yields (38%, 15%, and 16%, respectively) after chromatography.

Compounds **3**–**5** were readily formulated on the basis of standard analytical techniques, including the molecular ions observed in their field-desorption mass spectra. Each of the clusters exhibits a single ^1H NMR resonance in the hydride region between $\delta -12$ and -13, indicating equivalence of the two hydride ligands. For **3** and **4**, the hydride signal is split into a doublet by the phosphorus atom, with the coupling constant the same for each ($^3J(PH) = 3$ Hz). The magnitude of this coupling is in the range observed for three-bond phosphorus–hydrogen coupling in organic phosphates. The methyl protons of **4** show coupling to phosphorus ($^2J(PH) = 17$ Hz) with a value equal to that observed for the free acid ($^2J(PH) = 17.1$ Hz) [12]. In **3**, the P–C coupling constants for the phenyl ring, especially $^1J(PC)$, agree well with those reported for the free acid ($^1J(PC) = 186.5$ *vs.* 184.9 Hz, $^3J(PC) = 14.1$ *vs.* 15.0 Hz, $^2J(PC) = 9.1$ *vs.* 10.6 Hz, $^4J(PC) = 2.8$ *vs.* 3.3 Hz) [13].

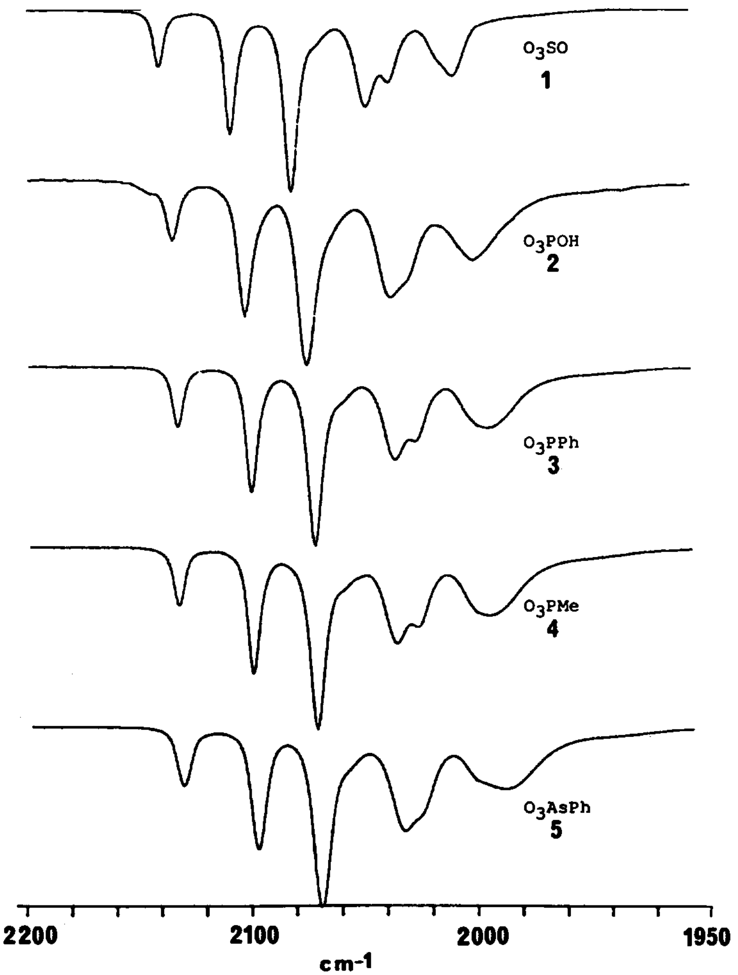

Fig. 1. Carbonyl region IR spectra for **1**–**5**. Spectra were recorded in dichloromethane.

The carbonyl stretching vibrations for **1**–**5** (see Fig. 1) are similar both in position and relative intensity, suggesting that all of these derivatives are isostructural. The relative position of the bands for each compound appear to depend on the basicity of the oxyanion ligand [14*]. If the bands for the structurally related compound $(\mu\text{-H})_2\text{Os}_3(\text{CO})_9(\mu_3\text{-S})$ (**6**) [15] are considered, an extended correlation can be developed, as shown in Fig. 2.

Oxyanion ligand vibrations

Carbon disulfide provides a clear window for examining the important oxyanion ligand vibrations of compounds **3**–**5** in solution. Solid/solution structure equivalence is shown by the excellent agreement between solid and solution bands, as shown in Fig. 3 for the two phosphonate compounds **3** and **4**.

---

* Reference number with an asterisk indicates a note in the list of references.

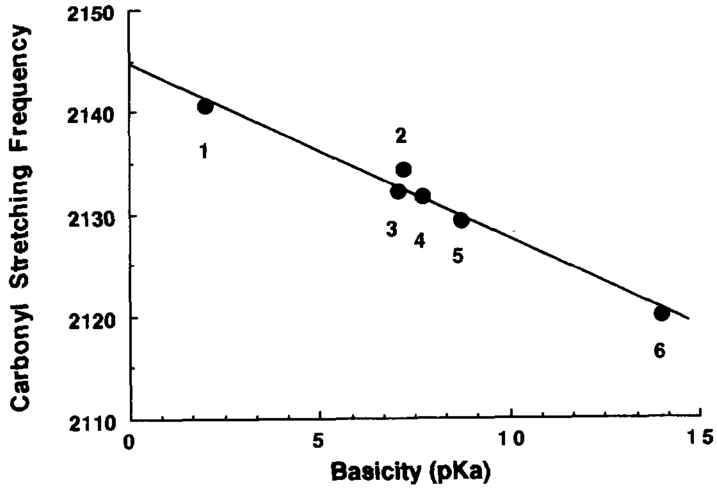

Fig. 2. Correlation of the *highest* carbonyl stretching frequency displayed by the compound $(\mu\text{-H})_2Os_3(CO)_9\mu_3\text{-X})$ with the p*K*a of HX-. Ionization constants from [14] and IR spectrum of $H_2Os_3(CO)_9S$ from [15].

We can make some assignments of the mid-range ligand vibrations for 3–5, including the E–O stretches, by comparison with those observed for the free acids (see Table 1) [16*]. In each instance, a notable difference between spectra for the

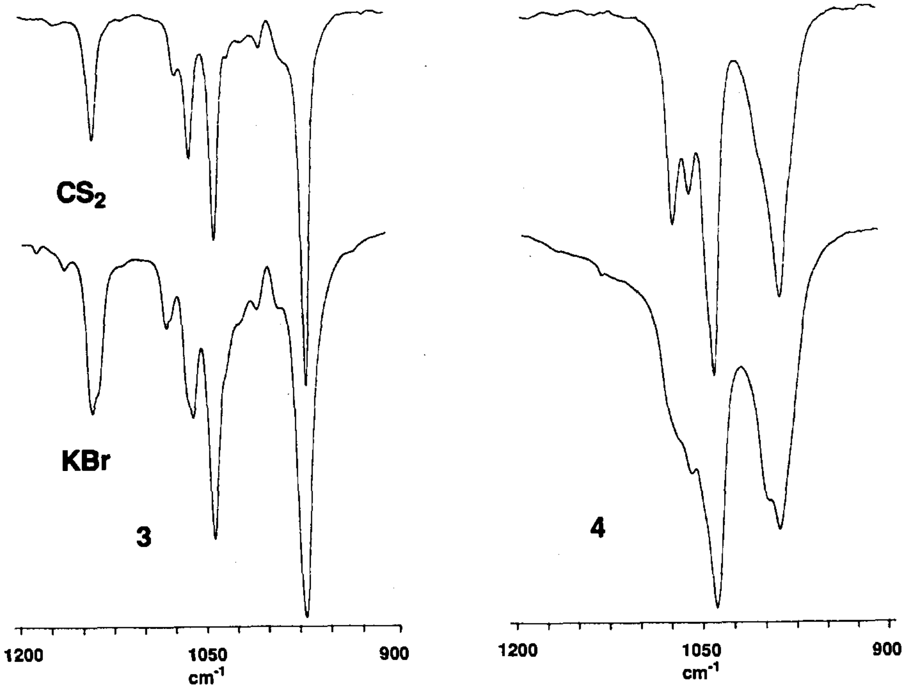

Fig. 3. E–O vibrational bands for phosphonate and arsonate ligands in clusters 3–5 in CS_2 and KBr.

Table 1

Selected vibrational bands for phosphonate and arsonate ligands in clusters 3–5 and the corresponding acids [a,b]

Compounds						Assignment
3	4	5	$PhPO_3H_2$ [b]	$MePO_3H_2$ [b]	$PhAsO_3H_2$ [b]	
	1308 (m) [a]			1316 (ms)		δ-CH_3
1440 (w)		1095 (m)	1150 (vs)		1100 (m)	"$\nu(C_{arom}E)$"
	1071 (m)		1181 (s)	1159 (ms)	890 (s)	"ν(E–O)"
1062 (m)	1059 (m)	837 (vs)	1023 (vs)	1011 (s)	845 (sh)	"ν(E–O)"
1042 (s)	1039 (vs)	815 (s)	1002 (s)	967 (s)	810 (vs)	"ν(E–O)"
968 (vs)	1001 (m)	738 (m)	944 (s)	936 (s)	783 (vs)	"ν(E–O)"
	987 (vs)					"ν(E–O)"

[a] Dispersed in KBr. [b] Free acid data from ref. 16.

free acids and the coordinated anions is the absence of a high energy E–O stretch in the latter. Such stretches are associated with E–O bonds having significant double bond character, consistent with the expected bond order reduction in the coordinated oxyanions. Each coordinated anion has local C_s symmetry and three E–O stretches are expected. For **3**, the P–O stretches likely correspond to the three bands observed at 1062 (m), 1042 (s), and 968 (vs) cm^{-1} in solution. The prominent bands at 1140 (m) cm^{-1} for **3** and 1095 (m) cm^{-1} for **5** correspond to similar bands in the free acids that have been assigned as C–E stretches, where the hydrocarbon substituent is an aromatic group. Given their relatively high energy, however, it is likely that these vibrational modes are mostly symmetric, in-plane C–H bending that is coupled with lower energy C–E stretching. A similar mode for the methyl group, the "umbrella" bending mode, is seen as 1308 (m) cm^{-1} in the spectrum of **4**, a position close to that in the free acid. Compound **4** exhibits more bands in the ν(PO) region that is expected by symmetry (see Table 1). It is probable that one of these bands is a P–C stretch but the methyl rocking mode may also occur in this range, since the situation for the H_3C–PO_3 ligand is similar to that encountered in assigning the modes for the ethylidyne ligand in $H_3Os_3(CO)_9(\mu_3\text{-}C\text{-}CH_3)$ [17] and related compounds. Only two of the As–O stretches in **5** can be confidently assigned, *i.e.*, 837 (vs) and 815 (s) cm^{-1}. The third band may be that at 738 (m) cm^{-1}, but this is the region also occupied by C–H bending modes (*ca.* 690 to 750 cm^{-1}) [16]. For $[Mn_3(1,4,7\text{-triazacyclononane})_3(\mu_3\text{-}O_3AsO)]Br_3$, IR bands are observed at 880 and 800 cm^{-1} [3].

Solid State Structure of $(\mu\text{-}H)_2Os_3(CO)_9(\mu_3,\eta^3\text{-}O_3PPh)$ (3)

Compound **3** can be obtained as a crystalline material from concentrated methanol solution and was examined by X-ray diffraction. Unfortunately, the quality of the crystallographic results was severely impaired by several disorder problems. Nevertheless, the gross structural features observed show the expected μ_3,η^3-coordination of the phenylphosphonate group to the triosmium framework.

Variable temperature ^{13}C NMR study

Compound **3** has been studied by variable temperature ^{13}C NMR spectroscopy (see Fig. 4). At low temperature (−40°C), five resonances of relative intensity 2:2:2:1:2 are observed in the carbonyl region. This pattern is consistent with the

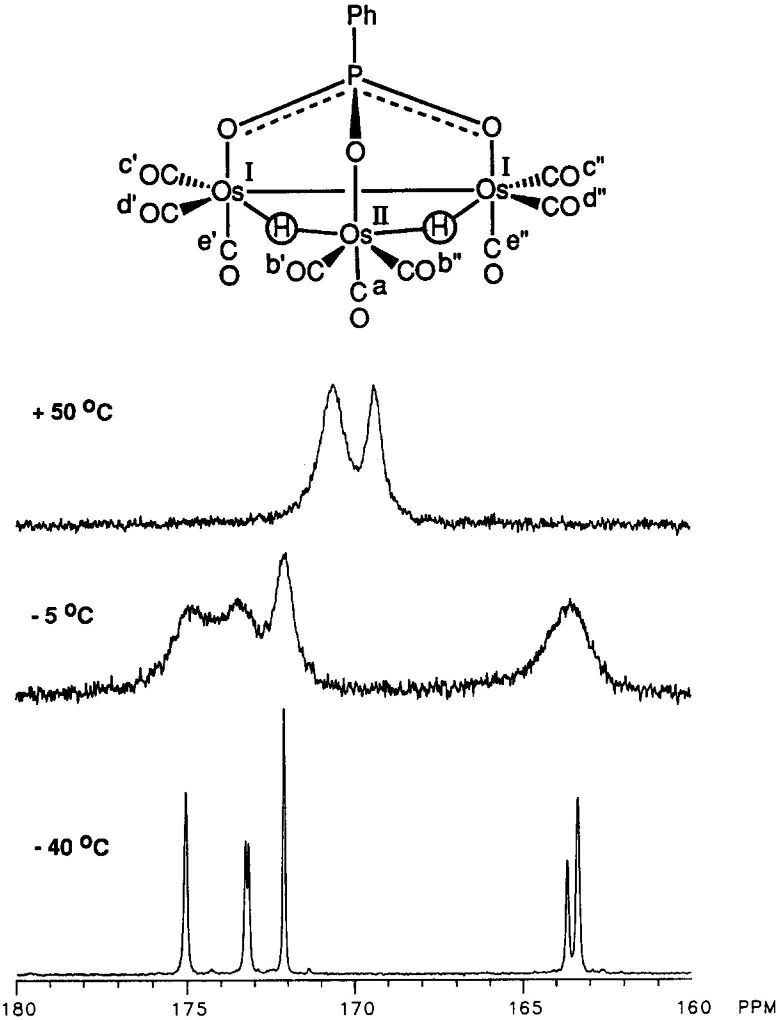

Fig. 4. Variable temperature ^{13}C {^1H} NMR spectra for **3** in chloroform-*d*.

expected molecular symmetry (C_s). Only the resonance at δ 173.22 shows strong coupling to ^{31}P (7.2 Hz).

Assignments of these resonances to specific carbonyls have been made. Given its unit intensity, the resonance at δ 163.66 can be assigned to CO^a (see Fig. 4). When ^1H coupled, the resonance at δ 163.35 is split into a doublet of multiplets (*trans*-^2J(CH) = 12.8 Hz and poorly resolved weak *cis*-^2J(CH) compounded by possible ^3J(PC) and *cis*-^2J(CC) of similar magnitude) and, consequently, is assigned to CO^b. CO^c are assigned to the δ 175.03 peak as they show strong ^1H coupling (*trans*-^2J(CH) = 6.3 Hz) indicating a *trans* relationship. The resonance at δ 172.11 shows no ^1H coupling, a feature which appears indicative of axial CO coordination, and is assigned to CO^e (further evidence in support of this assignment is provided by line broadening and signal averaging as described below). CO^d are assigned by default to the δ 173.22 resonance and show small ^1H coupling (*cis*-^2J(CH) = 3.3 Hz) in addition to the above mentioned ^{31}P coupling (7.2 Hz).

At elevated temperature (+50°C), two carbonyl resonances of relative intensity 3C:6C are observed at δ 169.4 and 170.6. Two mechanisms are possible that can explain this observed CO exchange: local CO scrambling or hydride migration. Local CO scrambling would interchange carbonyls a and b as well as carbonyls c, d, and e, giving rise to exchange averaged signals at about δ 163.5 (3C) and δ 173.5 (6C). These values are in poor agreement with those observed and, consequently, local CO scrambling as the low energy exchange process is unlikely.

On the other hand, hydride migration, which exchanges carbonyls a and e as well as b, c, and d, should result in exchange averaged signals at about δ 169.3 (3C) and 170.5 (6C), values which are in excellent agreement with those observed. Reversing the assignments for carbonyls d (δ 173.22 → 172.11) and e (δ 172.11 → 173.22), for which assignment from coupling data was inconclusive, results in poorer agreement (δ 170.0 (3C), δ 170.2 (6C)), lending support to the original assignments.

Further support of the original assignments and of hydride migration is provided by line broadening. Moving a hydride from the Os_I–Os_{II} metal–metal bond to the adjacent metal–metal bond (Os_I–$Os_{I'}$) interchanges the labels for the carbonyls in the following manner: $a \rightarrow e'$, $e'' \rightarrow a$, $e' \rightarrow e''$, $d' \rightarrow c''$, $d'' \rightarrow b'$, $c'' \rightarrow b''$, $c' \rightarrow d''$, $b' \rightarrow c'$, and $b'' \rightarrow d'$. As can be seen, in only one instance ($e' \rightarrow e''$) is a carbonyl not changed into a magnetically distinct carbonyl. Since line broadening is directly proportional to the rate of spin transfer in an exchange process, carbonyls e′ and e″ (which undergo only 50% interchange with each hydride hop) are expected to broaden more slowly than the others. The resonance at δ 172.11 has indeed broadened least at temperatures where the exchange process has begun (−5°C in Fig. 4), confirming its assignment to carbonyls e.

Preparation and characterization of $(\mu\text{-H})Os_3(CO)_{10}(\mu,\eta^2\text{-}O_2PPh_2)$

The reactive compounds $Os_3(CO)_{10}(S)_2$ ($S = C_8H_{14}, NCCH_3$) [18,19] have proved useful for the synthesis of various oxyanion ligand triosmium cluster derivatives, including $(\mu\text{-H})Os_3(CO)_{10}(\mu,\eta^2\text{-}O_2CH)$ [20], $(\mu\text{-H})Os_3(CO)_{10}(\mu\text{-OSiEt}_3)$ [21], and $(\mu\text{-H})Os_3(CO)_{10}[(\mu\text{-O})Si_7O_{10}(C_6H_{11})_7]$ [22]. Our attempts to prepare an analogous decarbonyl derivative from $PhPO_3H_2$ were not successful. However, the reaction of either $Os_3(CO)_{10}(NCCH_3)_2$ or $Os_3(CO)_{10}(C_8H_{14})_2$ with Ph_2PO_2H proceeds in THF solution at 55–60°C to give $(\mu\text{-H})Os_3(CO)_{10}(\mu,\eta^2\text{-}O_2PPh_2)$. The product was purified by chromatography on silica gel and isolated in *ca.* 60% yield. The ^1H NMR spectrum revealed one hydride ligand at δ −10.47 and ten aromatic hydrogens at δ 7.2–7.7. The hydride ligand in carboxylate derivatives of the type $(\mu\text{-H})Os_3(CO)_{10}(\mu,\eta^2\text{-}O_2CR)$ has a very similar chemical shift (δ 10.28 and 10.42, for $R = H, CH_3$, respectively) [23]. The hydride ligand appeared as a doublet due to coupling to phosphorus ($^3J(PH) = 8.7$ Hz). This coupling is considerably larger than that observed for $(\mu\text{-H})_2\text{-}Os_3(CO)_9(\mu_3,\eta^3\text{-}O_3PPh)$ ($^3J(PH) = 3$ Hz), which may be due to a more favorable P–O–Os–H dihedral angle.

It has been reported that $Ru_3(CO)_{12}$ reacts sequentially with excess Ph_2PO_2H followed by PPh_3 in refluxing THF to give the dimeric species $Ru_2(O_2PPh_2)_2(CO)_4(PPh_3)_2$ [24]. We expected that $(\mu\text{-H})Os_3(CO)_{10}(\mu,\eta^2\text{-}O_2PPh_2)$ might be an intermediate stage in the formation of the dinuclear osmium analog. For instance, $Os_2(CO)_6(\mu\text{-OAc})_2$ is formed by heating $H_2Os_3(CO)_9(OAc)_2$ with excess acetic acid [11]. However, no reaction of $(\mu\text{-H})Os_3(CO)_{10}(\mu,\eta^2\text{-}O_2PPh_2)$ with excess

Ph_2PO_2H in refluxing THF was observed, and attempted reaction in refluxing dioxane gave only $H_4Os_4(CO)_{12}$. Substitution of CO occurs in the presence of PPh_3 in refluxing THF to give $(\mu\text{-H})Os_3(CO)_9(PPh_3)(\mu,\eta^2\text{-}O_2PPh_2)$ as a mixture of isomers identified by mass spectroscopy. Similarly, phosphite substituted carboxylate derivatives such as $(\mu\text{-H})Os_3(CO)_9(P(OMe)_3)(\mu,\eta^2\text{-}O_2CCH_3)$ have been reported [25].

Solid-state molecular structure of $(\mu\text{-H})Os_3(CO)_{10}(\mu,\eta^2\text{-}O_2PPh_2)$

Two crystallographically independent molecules, A and B, of $(\mu\text{-H})Os_3(CO)_{10}$-$(\mu,\eta^2\text{-}O_2PPh_2)$ are found in the solid state. They differ principally in the positions of the phenyl rings, but most important bond distances and angles vary only slightly. Selected bond distances and angles are given in Table 4. A diagram of molecule A is shown in Fig. 5.

The molecule possesses approximate C_s symmetry and consists of a triangular Os_3 core to which are bound ten terminal CO ligands, a bridging bidentate Ph_2PO_2 ligand, and a bridging hydride ligand. The position of the hydride ligand was not located directly but its position can be deduced as bridging the Os1–Os2 edge roughly in the Os_3 equatorial plane because of (i) the elongated Os1–Os2 distance (2.945(avg)Å) compared with the Os1–Os3 distances (2.869(avg)Å), and (ii) the splaying of two equatorial CO ligands away from this position as evidenced by the angles Os2–Os1–C13 (118.7(avg)°) and Os1–Os2–C22 (119.0(avg)°). These changes are in accord with the expected consequences of a bridging hydride ligand in such a position [26].

The Ph_2PO_2 ligand bridges the Os1–Os2 edge and is bound in a diaxial bidentate fashion. The axial nature of phosphinate coordination to the metal framework is clear from the angle between the O14–Os1–Os2–O24 "coordination plane" and the Os_3 plane (93.74 and 94.08° for A and B, respectively). In contrast, this angle is more obtuse in carboxylate derivatives such as $(\mu\text{-H})Os_3(CO)_{10}(\mu,\eta^2\text{-}O_2CH)$ [20] and $(\mu\text{-H})Os_3(CO)_{10}(\mu,\eta^2\text{-}O_2CCH_3)$ [27] (98.6 and 97.0°, respectively). The nearness of this angle to 90° is all the more surprising given the fact the PPh_2 moiety is bent outwards from the "coordination plane" as evidenced by the angle between the O–Os–Os–O plane and the O–P–O plane (38.84 and 33.90° for A and B, respectively). This tilting away is evidently the result of a steric interaction between a phenyl ring and the adjacent axial CO ligand. The O14–P1–O24 "bite" distance is a good match for the Os–H–Os distance, resulting in positions for the coordinating oxygen atoms of the phosphinate ligand that are nearly on top of the corresponding osmium atoms, as evidenced by Os1–Os2–O24 and Os2–Os1–O14 angles of 85.0(3) and 83.8(3)°, respectively. The Os–O distances (2.15(avg) Å) are comparable to those observed in other oxyligand clusters, such as $(\mu\text{-H})Os_3(CO)_{10}(\mu,\eta^2\text{-}O_2CH)$ (2.16(avg) Å) [20] and $(\mu\text{-H})_2Os_3(CO)_9(\mu_3,\eta^3\text{-}O_3SO)$ (2.13(avg)Å) [1].

Experimental

General procedures

$(\mu\text{-H})_3Os_3(CO)_9(\mu_3\text{-CH})$ [10], $Os_3(CO)_{10}(C_8H_{14})$ [18], and $Os_3(CO)_{10}(CH_3CN)_2$ [19] were prepared according to literature methods. F_3CSO_3H (Aldrich) was vacuum distilled. $PhPO_3H_2$ (Aldrich, 98%), $MePO_3H_2$ (Aldrich, 98%), $PhAsO_3H_2$

(Aldrich, 97%), and Ph_2PO_2H (Aldrich, 99%) were dried *in vacuo* at elevated temperature (*ca.* 70°C). Acid treated Fluorosil columns were prepared by loading Fluorosil, slurried in methanol, into a glass column (1 cm inside diameter) to a bed height of 24 cm and then washing the column successively with methanol/acetic acid (50 mL, 4/1), methanol (50 mL), and dichloromethane (50 mL).

Elemental analyses were performed by the Microanalytical Laboratory of the School of Chemical Sciences. ^1H NMR spectra were obtained on either a Nicolet NT-360 spectrometer (360 MHz) or a GE QE-300 spectrometer (300 MHz) and were referenced to residual proton resonances in the deuterated solvents. ^{13}C NMR spectra were obtained on a GE QE-300 spectrometer (75.5 MHz) and were referenced to appropriate solvent resonances (dichloromethane-d_2: δ 53.8, chloroform-d; δ 77.0). IR spectra were recorded on a Perkin–Elmer 1750 Fourier transform spectrometer. Mass spectra were obtained by the staff of the Mass Spectroscopy Laboratory of the School of Chemical Sciences using a Varian MAT-731 for field desorption ionization.

$(\mu\text{-}H)_2Os_3(CO)_9(\mu_3,\eta^3\text{-}O_3PPh)$ (3). Solid $(\mu\text{-H})_3Os_3(CO)_9(\mu_3\text{-CH})$ (65.0 mg, 0.0775 mmol) was dissolved in F_3CSO_3H (0.4 mL) with accompanying gas evolution. A solution of $PhPO_3H_2$ (0.775 g) in methanol (0.4 mL) was then added with thorough mixing. After *ca.* 15 min, water (10 mL) was added with thorough mixing and the resulting precipitate collected, washed with water (4 × 10 mL), and dried *in vacuo*. This precipitate was dissolved in dichloromethane, and loaded onto an SiO_2 dry-packed column; the yellow band that eluted with dichloromethane was collected and the solvent evaporated. Crystallization of the residue from methanol at −15°C gave **3** as pale yellow needles containing methanol of crystallization (*ca.* 1 mole methanol/7 moles **3** as determined by ^1H NMR). These needles were used in the diffraction study. Overnight storage *in vacuo* gave **3** free of methanol and reported below are the spectroscopic and analytical data for this material. Yield: 28.9 mg, 0.0295 mmol, 38%.

Anal. Found: C, 18.42; H, 0.70. $C_{15}H_7O_{12}Os_3P$ calcd.: C, 18.37; H, 0.72%. ^1H NMR (CD_2Cl_2, *ca.* 20°C): δ 7.54–7.27 (m, 5H), −12.57 (d, $^3J(PH) = 3$ Hz, 2H). IR (CH_2Cl_2): ν(CO)2132 (m), 2099 (s), 2071 (vs), 2036 (s), 2027 (m), 1998 (m) cm^{-1}. IR (KBr, 1600–800 cm^{-1}): 1440 (w),1141 (m), 1080 (w), 1061 (m), 1043 (s), 1007 (vw), 969 (vs) cm^{-1}. IR (CS_2, 1200–900 cm^{-1}): 1140 (m), 1073 (w), 1062 (m), 1042 (s), 1005 (vw), 968 (vs) cm^{-1}. MS (field desorption, ^{192}Os): m/z 986 (M^+).

$(\mu\text{-}H)_2Os_3(CO)_9(\mu_3,\eta^3\text{-}O_3PMe)$ (4). Solid $(\mu\text{-H})_3Os_3(CO)_9(\mu_3\text{-CH})$ (73.8 mg, 0.0880 mmol) was dissolved in F_3CSO_3H (0.35 mL) with accompanying gas evolution. The resulting yellow solution was cooled in ice/water and $MePO_3H_2$ (0.826 g) in methanol (0.4 mL) added with thorough mixing. After 40 min, water (10 mL) was added with thorough mixing, and the resulting yellow precipitate was collected, washed with water (4 × 10 mL), and dried *in vacuo*. This solid was then dissolved in dichloromethane and loaded onto an acid treated Fluorosil column. After complete elution of any dichloromethane mobile bands, the column was eluted with methanol/dichloromethane (5/95) and the mobile yellow band collected. The eluate was taken to dryness and the resulting residue recrystallized from methanol at −15°C to give **4** as a yellow crystalline solid. Yield: 12.2 mg, 0.0133 mmol, 15%.

Anal. Found: C, 13.16; H, 0.54. $C_{10}H_5O_{12}Os_3P$ calcd.: C, 13.07; H, 0.55%. ^1H NMR (CD_2Cl_2): δ 1.13 (d, $^2J(PH) = 17$ Hz, 3H), −12.68 (d, $^3J(PH) = 3$ Hz, 2H).

IR (CH_2Cl_2): ν(CO)2132 (m), 2099 (s), 2070 (vs), 2036 (s), 2026 (m), 1998 (m) cm^{-1}. IR (KBr, 1600–800 cm^{-1}): 1308 (w), 1069 (sh), 1059 (m), 1039 (s), 999 (m), 987 (m) cm^{-1}. IR (CS_2, 1200–900 cm^{-1}): 1300 (w), 1071 (m), 1059 (m), 1001 (sh), 1039 (s), 987 (m) cm^{-1}. MS (field desorption, ^{192}Os): m/z 924 (M^+).

(μ-H)$_2$Os$_3$(CO)$_9$(μ_3,η^3-O$_3$AsPh) (5). Solid (μ-H)$_3$Os$_3$(CO)$_9$(μ_3-CH) (76.9 mg, 0.0917 mmol) was dissolved in F_3CSO_3H (0.35 mL) with accompanying gas evolution. The resulting yellow solution was cooled in ice/water, and $PhAsO_3H_2$ (0.685 g), slurried in methanol (0.6 mL), was added with thorough mixing. The reaction mixture was allowed to stand at 25°C for 15 min. Water (10 mL) was added and the resulting yellow precipitate was collected, washed with water (4 × 10 mL), and dried *in vacuo*. This solid was dissolved in dichloromethane and loaded onto an acid treated Fluorosil column. After complete elution of dichloromethane mobile bands, the column was eluted with methanol/dichloromethane (1/9) and the mobile yellow band collected. This eluate was evaporated and the residue crystallized from diethylether. Compound 5 was obtained as orange-yellow needles. Yield: 15.5 mg, 0.0151 mmol, 16%.

Anal. Found: C, 17.85; H, 0.62. $C_{15}H_7AsO_{12}Os_3$ calcd.: C, 17.58; H, 0.69%. ^1H NMR (CD_2Cl_2): δ 7.58–7.41 (m, 5H), −12.25 (2H). IR (CH_2Cl_2): ν(CO) 2129 (m), 2097 (s), 2068 (vs), 2032 (s), 2025 (m), 1995 (m) cm^{-1}. IR (KBr, 1600–640 cm^{-1}): 1443 (m), 1095 (m), 838 (s), 829 (sh), 817 (sh), 743 (m), 705 (sh), 697 (sh), 692 (m) cm^{-1}): IR (CS_2, 900–660 cm^{-1}): 1096 (w), 837 (vs), 815 (s), 738 (m), 720 (vw), 689 (m) cm^{-1}. MS (field desorption, ^{192}Os): m/z 1030 (M^+).

X-ray crystallographic study of (μ-H)$_2$Os$_3$(CO)$_9$(μ_3,η^3-O$_3$PPh) (3). $Os_3PO_{12}C_{15}H_7$, MW 980.79, hexagonal, $P6_3/m$, a = 18.940(10) Å, $b = a$, c = 11.483(6) Å, $\alpha = \beta = 90°$, $\gamma = 120°$, $V = 3569(4)$ Å^3, $Z = 6$, $\rho(calc) = 2.738$ g cm^{-3}, T = 298 K, $\mu(Mo\text{-}K_\alpha) = 161.2$ cm^{-1}. The crystal did not uniformly extinguish plane-polarized light and showed a weak diffraction pattern with a broad mosaic spread. The structure was solved by direct methods (SHELX-76) and refined by least squares-difference Fourier calculations. Final agreement factors were $R = 0.090$; $R_w = 0.091$. The accuracy of the results were limited by a disordered phenyl group and probable disordered solvent molecules in the lattice. The geometric features of the molecule were as expected, with reasonable Os–Os (2.968 Å avg) and Os–O (2.10 Å avg) distances.

Synthesis of (μ-H)Os$_3$(CO)$_{10}$(μ,η^2-O$_2$PPh$_2$). To Ph_2PO_2H (15.4 mg, 0.0706 mmol) in a Schlenk tube was added $Os_3(CO)_{10}(C_8H_{14})_2$ (75.3 mg, 0.0703 mmol) in cyclooctene. The cyclooctene was removed at reduced pressure, THF (3 mL) was

Table 2

Summary of crystallographic data for (μ-H)Os$_3$(CO)$_{10}$(μ,η^2-O$_2$PPh$_2$)

Formula	2($Os_3PO_{12}C_{22}H_{11}$)	Formula wt	2(1068.90)
a (Å)	16.549(11)	Space group	$P2_1/n$ (No. 14)
b (Å)	15.533(7)	T (°C)	−75
c (Å)	20.376(9)	λ (Å)	0.71073
β	98.40(5)°	ρ_{calcd} (g cm^{-3})	2.74
V (Å^3)	5182(8)	μ (cm^{-1})	148.12
Z	8(4)	Trans. factors	0.023–0.122
R	0.044	R_w	0.058

Table 3

Final positional parameters for the non-hydrogen atoms of $(\mu\text{-H})Os_3(CO)_{10}(\mu,\eta^2\text{-}O_2PPh_2)$

	x	*y*	*z*
Molecule A			
Os1	0.32798(4)	0.02779(5)	0.81795(4)
Os2	0.26787(4)	−0.15112(5)	0.80304(4)
Os3	0.17451(4)	−0.02009(5)	0.85654(4)
P1	0.2570(3)	−0.0321(3)	0.6724(2)
O11	0.4154(8)	0.0001(9)	0.9560(7)
O12	0.2923(8)	0.2120(9)	0.8524(7)
O13	0.4942(8)	0.0657(9)	0.7761(7)
O14	0.2652(7)	0.0452(8)	0.7181(6)
O21	0.3285(9)	−0.204(1)	0.9440(9)
O22	0.3784(8)	−0.2885(9)	0.7574(7)
O23	0.1200(9)	−0.269(1)	0.7987(8)
O24	0.2254(7)	−0.1123(8)	0.7028(6)
O31	0.2528(9)	−0.048(1)	1.0009(8)
O32	0.0243(10)	−0.126(1)	0.8741(9)
O33	0.1363(8)	0.1617(10)	0.8994(7)
O34	0.0843(8)	0.0121(9)	0.7166(7)
C11	0.380(1)	0.011(1)	0.9034(9)
C12	0.3045(10)	0.143(1)	0.8387(9)
C13	0.4314(10)	0.052(1)	0.7894(9)
C21	0.308(1)	−0.181(1)	0.889(1)
C22	0.338(1)	−0.236(1)	0.770(1)
C23	0.176(1)	−0.224(1)	0.8018(10)
C31	0.225(1)	−0.040(1)	0.945(1)
C32	0.083(1)	−0.084(1)	0.869(1)
C33	0.149(1)	0.092(1)	0.8829(9)
C34	0.123(1)	−0.004(1)	0.7660(10)
C71	0.188(1)	−0.009(1)	0.5997(10)
C72	0.160(1)	−0.074(1)	0.559(1)
C73	0.107(1)	−0.059(1)	0.498(1)
C74	0.091(1)	0.026(1)	0.479(1)
C75	0.119(1)	0.091(2)	0.520(1)
C76	0.168(1)	0.077(1)	0.581(1)
C81	0.353(1)	−0.051(1)	0.6431(9)
C82	0.4020(10)	0.014(1)	0.6329(9)
C83	0.474(1)	0.001(1)	0.6062(10)
C84	0.495(1)	−0.080(1)	0.593(1)
C85	0.447(1)	−0.151(1)	0.604(1)
C86	0.377(1)	−0.137(1)	0.632(1)
Molecule B			
Os4	0.84139(4)	0.21106(5)	0.71017(4)
Os5	0.78417(4)	0.39034(5)	0.70325(4)
Os6	0.71577(5)	0.26538(5)	0.60645(4)
P2	0.7210(3)	0.2665(3)	0.8130(2)
O41	0.9711(9)	0.243(1)	0.6253(8)
O42	0.8192(9)	0.030(1)	0.6563(8)
O43	0.9773(10)	0.149(1)	0.8166(9)
O44	0.7513(7)	0.1910(8)	0.7763(7)
O51	0.8996(10)	0.451(1)	0.6132(9)
O52	0.8544(8)	0.5238(10)	0.8069(8)
O53	0.6470(9)	0.508(1)	0.6415(8)
O54	0.7059(7)	0.3474(8)	0.7710(6)

Table 3 (continued)

	x	y	z
Molecule B			
O61	0.8378(10)	0.311(1)	0.5098(9)
O62	0.5915(9)	0.383(1)	0.5272(8)
O63	0.6823(10)	0.093(1)	0.5382(9)
O64	0.5826(8)	0.2170(9)	0.6916(7)
C41	0.919(1)	0.231(1)	0.656(1)
C42	0.826(1)	0.097(1)	0.677(1)
C43	0.927(1)	0.174(1)	0.781(1)
C51	0.854(1)	0.430(1)	0.648(1)
C52	0.830(1)	0.471(1)	0.7692(10)
C53	0.700(1)	0.464(1)	0.664(1)
C61	0.795(1)	0.297(1)	0.550(1)
C62	0.638(1)	0.338(1)	0.556(1)
C63	0.695(1)	0.156(1)	0.565(1)
C64	0.634(1)	0.233(1)	0.663(1)
C91	0.6298(10)	0.242(1)	0.8436(8)
C92	0.562(1)	0.299(1)	0.832(1)
C93	0.493(1)	0.290(1)	0.8639(10)
C94	0.492(1)	0.224(1)	0.905(1)
C96	0.624(1)	0.175(1)	0.8880(10)
C95	0.557(1)	0.162(2)	0.916(1)
C101	0.790(1)	0.285(1)	0.8895(9)
C102	0.843(1)	0.219(1)	0.9160(10)
C103	0.887(1)	0.226(1)	0.978(1)
C104	0.879(1)	0.299(1)	1.014(1)
C105	0.830(1)	0.364(1)	0.988(1)
C106	0.784(1)	0.358(1)	0.9272(10)

added, and the reaction mixture was heated in an oil bath maintained at 55–60°C for 1.5 h. The color turned from yellow to orange-brown. The progress was monitored by IR and analytical TLC until the reaction was complete. The solvent was removed at reduced pressure, and the residue was subjected to TLC (n-hexane/dichloromethane, 10:1). Five well separated bands were observed and the prominent middle band of $(\mu\text{-H})Os_3(CO)_{10}(\mu,\eta^2\text{-}O_2PPh_2)$ was recovered and recrystallized from n-pentane. Yield: 42.8 mg, 0.0401 mmol, 57%. Crystals suitable for X-ray diffraction deposited from n-pentane/n-hexane solution at 25°C. A comparable yield was obtained starting with $Os_3(CO)_{10}(NCCH_3)_2$.

Anal. Found: C, 25.14; H, 1.12 Calcd. for $C_{22}H_{11}O_{12}Os_3P$: C, 24.72; H, 1.04%. IR (C_6H_{12}): ν_{CO} 2113(w), 2070(s), 2064(sh), 2024(vs), 2004(m), 1982(m), 1951(w) cm^{-1}. ^1H NMR $(CDCl_3)$: δ 7.2–7.7 (m, 10H), -10.47 (d, $^3J_{PH} = 8.7$ Hz, 1H). MS (field desorption, ^{192}Os): m/z 1074 (M^+).

X-ray crystallographic study of $(\mu\text{-H})Os_3(CO)_{10}(\mu,\eta^2\text{-}O_2PPh_2)$. The crystallographic data set was collected at -75°C on an Enraf-Nonius CAD4 κ-axis diffractometer using a ω/θ scan mode and Mo-K_α radiation. The transparent yellow prismatic crystal was mounted using oil (Paratone-N, Exxon) to a thin glass fiber with the (0 -6 -5) scattering plane roughly normal to the spindle axis. Crystal data, and details for the data collection and refinement are shown in Table 2. There was no change in the appearance of the sample during the experiment. The

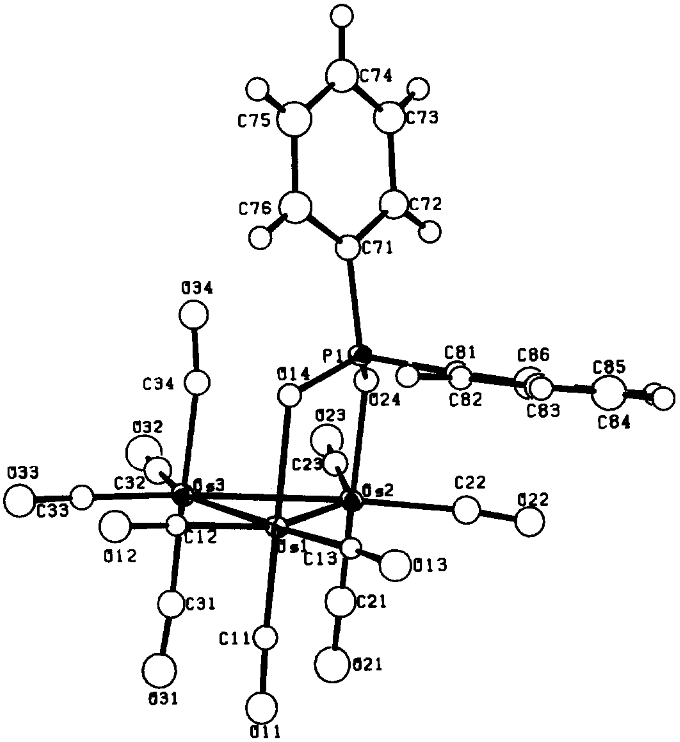

Fig. 5. ORTEP diagram of $(\mu\text{-H})_2Os_3(CO)_{10}(\mu,\eta^2\text{-}O_2PPh_2)$ (molecule A) showing the atom labeling scheme.

Table 4

Selected bond distances (Å) and angles (°) for $(\mu\text{-H})Os_3(CO)_{10}(\mu,\eta^2\text{-}O_2PPh_2)$

	Molecule A	Molecule B		Molecule A	Molecule B
Bond distances					
Os1–Os2	2.952(1)	2.938(1)	P1–O14	1.51(1)	1.52(1)
Os1–Os3	2.8645(10)	2.866(1)	P1–O24	1.52(1)	1.52(1)
Os2–Os3	2.865(1)	2.879(1)	P1–C71	1.772(2)	1.76(2)
Os1–O14	2.16(1)	2.17(1)	P1–C81	1.80(2)	1.82(2)
Os2–O24	2.15(1)	2.13(1)			
Bond angles					
Os2–Os1–Os3	59.00(2)	59.45(3)	O14–Os1–C11	178.7(6)	178.1(8)
Os1–Os2–Os3	58.97(2)	59.04(3)	O24–Os2–C21	177.6(7)	177.5(7)
Os1–Os3–Os2	62.03(3)	61.52(3)	Os3–Os2–C23	87.4(6)	85.9(6)
Os2–Os1–O14	85.0(3)	85.4(3)	Os3–Os1–C12	88.0(5)	88.2(6)
Os1–Os2–O24	83.8(3)	83.9(3)	C12–Os1–C13	96.1(7)	91.7(9)
Os3–Os1–O14	88.1(3)	90.6(3)	C22–Os2–C23	96.1(8)	95.0(8)
Os3–Os2–O24	92.5(3)	91.0(3)	C32–Os3–C33	103.8(8)	102.7(9)
O14–P1–O24	114.0(7)	113.6(7)	C33–Os3–Os1	94.7(5)	97.4(6)
O14–P1–C71	109.8(8)	112.0(8)	C32–Os3–Os2	99.4(6)	98.2(6)
O24–P1–C71	107.0(8)	107.3(7)	Os1–Os2–C22	117.9(6)	120.0(6)
P1–O14–Os1	117.9(7)	120.1(7)	Os2–Os1–C13	116.8(5)	120.6(6)
P1–O24–Os2	122.2(7)	123.9(7)			

structure was solved by direct methods (SHELXS-86), and correct positions for the osmium and phosphorus atoms were deduced from an E-map. Subsequent least squares-difference Fourier calculations revealed positions for the remaining non-hydrogen atoms. Hydrogen atoms were included as fixed contributions in "idealized" positions. In the final cycle of least squares, anisotropic thermal coefficients were refined for the osmium and phosphorus atoms, independent isotropic thermal coefficients were refined for all non-hydrogen atoms, a common isotropic thermal parameter was varied for the hydrogen atoms, and an isotropic extinction parameter was refined. Successful convergence was indicated by the maximum shift/error for the final cycle. The highest peaks in the final difference Fourier map were in the vicinity of the heavy atoms. Positional parameters are listed in Table 3, and selected bond distances and angles are given in Table 4.

Acknowledgements

This research was supported by National Science Foundation grant DMR 89-20538 to the Materials Research Laboratory at the University of Illinois.

References and notes

1 R.L. Keiter, D.S. Strickland, S.R. Wilson and J.R. Shapley, J. Am. Chem. Soc., 108 (1986) 3846.

2 (a) R. Beckett, and B.F. Hoskins, J. Chem. Soc., Dalton Trans. (1972) 291; (b) J. Estienne, Acta Crystallogr., Sect. C, 41, (1985) 338; (c) M. Irmler and G. Meyer, Naturwissenschaften, 75 (1988) 308; (d) W. Clegg, J. Errington, D.C.R. Hockless, A.D. Glen, D.G. Richards, J. Chem. Soc., Chem. Commun., (1990) 1565.

3 K. Wieghardt, U. Bossek, B. Nuber, J. Weiss, S. Gehring and W. Haase, J. Chem. Soc., Chem. Commun., (1988) 1145.

4 (a) G. Huan, V.W. Day, A.J. Jacobson and D.P. Goshorn, J. Am. Chem. Soc. 113 (1991) 3188; (b) G.B. Jameson, M.T. Pope and S.H. Wasfi, J. Am. Chem. Soc. 107 (1985) 4911; (c) J.K. Stalick and C.O. Quicksall, Inorg. Chem. 15 (1976) 1577.

5 G. Cao, V.M. Lynch, J.S. Swinnea and T.E. Mallouk, Inorg. Chem., 29 (1990) 2112, and references therein.

6 J.G. Ekerdt, K.J. Klabunde, J.R. Shapley, J.M. White and J.T. Yates, Jr., J. Phys. Chem., 92 (1988) 6182.

7 M.K. Templeton and W.H. Weinberg, J. Am. Chem. Soc., 107 (1985) 97.

8 M.A. Henderson and J.M. White, J. Am. Chem. Soc., 110 (1988) 6939.

9 (a) M.A. Habib and J. O'M. Bockris, J. Electrochem. Soc., 32 (1985) 108; (b) M. Hourani and A. Wieckowski, J. Electroanal. Chem., 244 (1988) 147; (c) K. Kunimatsu, M.G. Samant, H. Seki and M.R. Philpott, J. Electroanal. Chem., 243 (1988) 203; (d) S. Manne, P.K. Hansma, J. Massie, V.B. Elings and A.A. Gewirth, Science, 251 (1991) 183.

10 R.B. Calvert and J.R. Shapley, J. Am. Chem. Soc., 99 (1977) 5225.

11 G.R. Frauenhoff, S.R. Wilson and J.R. Shapley, Inorg. Chem., 30 (1991) 78.

12 J.F. Nixon and R. Schmutzler, Spectrochim. Acta, 22 (1966) 565.

13 G. Ohms and G. Grossmann, Z. Anorg. Allg. Chem., 544 (1987) 232.

14 (a) H_2SO_4, H_2S and H_3PO_4: D.D. Perrin (Ed.) Ionisation Constants of Inorganic Acids and Bases in Aqueous Solution; Pergamon, Oxford, 1982; (b) $PhPO_3H_2$: H.H. Jaffe, L.D. Freedman and G.O. Doak, J. Am. Chem. Soc., 75 (1953) 2209; (c) $MePO_3H_2$: P.C. Crofts and G.M. Kosolapoff, J. Am. Chem. Soc., 75 (1953) 3379; (d) $PhAsO_3H_2$: C.O. Nuallain and S.O. Cinneide, J. Inorg. Nucl. Chem., 35 (1973) 2871.

15 B.F.G. Johnson, J. Lewis, D.A. Pippard, P.R. Raithby, G.M. Sheldrick and K.D. Rouse, J. Chem. Soc., Dalton Trans., (1979) 616.

16 (a) $PhPO_3H_2$: U. Dietze J. Prakt. Chem., 316 (1974) 485; (b) $MePO_3H$: H. Gerding, J.W. Maarsen and D.H. Zijp, Recl. Trav. Chim. Pays-Bas, 77 (1958) 361; (c) $PhAsO_3H_2$: U. Dietze, J. Prakt. Chem., 313 (1971) 889.

17 J.L. Coffer, H.G. Drickamer, J.T. Park, R.T. Roginski and J.R. Shapley, J. Phys. Chem., 94 (1990) 1981.
18 M. Tachikawa and J.R. Shapley, J. Organomet. Chem., 124 (1977) C19.
19 B.F.G. Johnson, J. Lewis and D.A. Pippard, J. Chem. Soc., Dalton Trans., (1981) 407.
20 J.R. Shapley, G.M. St. George, M.R. Churchill and F.J. Hollander, Inorg. Chem., 21 (1982) 3295.
21 (a) T.H. Walter, G.R. Frauenhoff, J.R. Shapley and E. Oldfield, Inorg. Chem., 27 (1988) 2651; (b) T.H. Walter, G.R. Frauenhoff, J.R. Shapley and E. Oldfield, Inorg. Chem., 30 (1991) 4732; (c) L.D'Ornelas, A. Choplin, J.M. Basset, L.-Y. Hsu and S. Shore, Nouv. J. Chim., 9 (1985) 155.
22 J.-C. Liu, S.R. Wilson, J.R. Shapley and F.J. Feher, Inorg. Chem., 29 (1990) 5138.
23 E.G. Bryan, B.F.G. Johnson and J. Lewis, J. Chem. Soc., Dalton Trans., (1977) 1328.
24 D.S. Bohle and H. Vahrenkamp, Inorg. Chem., 29 (1990) 1097.
25 E.J. Ditzel, B.F.G. Johnson and J. Lewis, J. Chem. Soc., Dalton Trans., (1987) 1293.
26 (a) M.R. Churchill, B.G. DeBoer and F.J. Rotella, Inorg. Chem., 15 (1976) 1843; (b) M.R. Churchill, Adv. Chem. Ser., 167 (1978) 36.
27 P.M. Lausarot, G.A. Vaglio, M. Valle, A. Tiripicchio, M.T. Camellini and P. Gariboldi, J. Organomet. Chem., 291 (1985) 221.